Journal of Pathology
J Pathol 2020; **250:** 440–451
Published online 25 February 2020 in Wiley Online Library (wileyonlinelibrary.com) DOI: 10.1002/path.5385

ORIGINAL PAPER

LIGHT/TNFSF14 regulates estrogen deficiency-induced bone loss

Giacomina Brunetti[1†*], Giuseppina Storlino[2†], Angela Oranger[2], Graziana Colaianni[2], Maria F Faienza[3], Giuseppe Ingravallo[4], Mariasevera Di Comite[1], Janne E Reseland[5], Monica Celi[6], Umberto Tarantino[6], Giovanni Passeri[7], Carl F Ware[8], Maria Grano[2‡] and Silvia Colucci[1‡]

[1] *Department of Basic and Medical Sciences, Neurosciences and Sense Organs, Section of Human Anatomy and Histology, University of Bari, Bari, Italy*
[2] *Department of Emergency and Organ Transplantation, Section of Human Anatomy and Histology, University of Bari, Bari, Italy*
[3] *Department of Biomedical Science and Human Oncology, Paediatric Unit, University of Bari, Bari, Italy*
[4] *Department of Emergency and Organ Transplantation, Pathology Section, University of Bari, Bari, Italy*
[5] *Department of Biomaterials, Institute for Clinical Dentistry, University of Oslo, Blindern, Oslo, Norway*
[6] *Department of Orthopedics and Traumatology, Tor Vergata University of Rome, Rome, Italy*
[7] *Department of Clinical and Experimental Medicine, University of Parma, Parma, Italy*
[8] *Laboratory of Molecular Immunology, Infectious and Inflammatory Disease Center, Sanford Burnham Prebys Medical Discovery Institute, La Jolla, California, USA*

**Correspondence to: G Brunetti, Department of Basic and Medical Sciences, Neurosciences and Sense Organs, Section of Human Anatomy and Histology, University of Bari, Piazza Giulio Cesare, 11, 70124 Bari, Italy. E-mail: giacomina.brunetti@uniba.it*

[†]GB and GS contributed equally to this work as co-first authors.
[‡]MG and SC contributed equally to this work as co-senior authors.

Abstract

Bone loss induced by ovariectomy is due to the direct activity on bone cells and mesenchymal cells and to the dysregulated activity of bone marrow cells, including immune cells and stromal cells, but the underlying mechanisms are not completely known. Here, we demonstrate that ovariectomy induces the T-cell co-stimulatory cytokine LIGHT, which stimulates both osteoblastogenesis and osteoclastogenesis by modulating osteoclastogenic cytokine expression, including TNF, osteoprotegerin, and the receptor activator of nuclear factor-κB ligand (RANKL). Predictably, LIGHT-deficient (*Tnfsf14*$^{-/-}$) mice are protected from ovariectomy-dependent bone loss, whereas trabecular bone mass increases in mice deficient in both LIGHT and T and B lymphocytes (*Rag*$^{-/-}$*Tnfsf14*$^{-/-}$) and is associated with an inversion of the TNF and RANKL/OPG ratio. Furthermore, women with postmenopausal osteoporosis display high levels of LIGHT in circulating T cells and monocytes. Taken together, these results indicate that LIGHT mediates bone loss induced by ovariectomy, suggesting that patients with postmenopausal osteoporosis may benefit from LIGHT antagonism.

Keywords: LIGHT/TNFSF14; ovariectomy; bone loss; postmenopausal osteoporosis; osteoimmunology; immune cells; osteoclasts; osteoblasts; TNF; RANKL/OPG

Received 2 September 2019; Revised 24 December 2019; Accepted 15 January 2020

No conflicts of interest were declared.

Introduction

LIGHT or TNFSF14 is an immunomodulatory cytokine and a member of the TNF superfamily. It is expressed by lymphocytes, monocytes, and granulocytes, and is primarily known for its critical role in immune functions [1–7]. Only recently has LIGHT's involvement in bone homeostasis and erosive bone diseases become increasingly evident [8–13]. Recently, we provided evidence for LIGHT's new role in maintaining skeletal physiology [10] after showing that trabecular bone mass was reduced in LIGHT-deficient (*Tnfsf14*$^{-/-}$) mice, an effect associated with increased osteoclast formation and activity along with reduced osteoprotegerin (OPG) expression by T and B cells in knockout mice [10]. The same mice also display impaired osteoblastogenesis activity, which is associated with low Wnt10b expression by $CD8^+$ T cells [10]. Additional evidence implicates LIGHT in mediating pathological bone remodeling in erosive rheumatoid arthritis [8], osteolytic multiple myeloma [9,13], chronic kidney disease, and arthropathy associated with alkaptonuria [12]. However, no link has been identified between bone loss from postmenopausal osteoporosis and LIGHT. Postmenopausal osteoporosis, a systemic skeletal disease in women characterized by low bone mass and increased fracture risk due to estrogen loss

[14], leads to alteration of bone cell activity both directly and indirectly through immune cells [14], but the underlying mechanisms are not completely known [15]. Indeed, estrogens modulate T- and B-cell activation, as well as the secretion of cytokines regulating bone turnover [15]. In mice, ovariectomy reproduces the acute effects of menopause, with bone resorption stimulating osteoclast formation [16] and increased lifespan [17–19]. Surprisingly, ovariectomy is also associated with increased bone formation, resulting in the attenuation of net bone loss [20]. Yet bone loss from ovariectomy appears to be a balance between the expansion of bone marrow stromal cells committed toward osteoblastic differentiation [20] and the limitation imposed by increased apoptosis [21,22], increased osteoclast lifespan [17,18], and cytokine production that inhibits bone formation, such as tumor necrosis factor-α (TNFα). These data indicate that several factors contribute to the imbalance between bone resorption and formation following ovariectomy [15]. Effects on bone turnover also involve T and B cells because ovariectomy fails to induce bone loss in nude mice deficient in T and B cells [23–26], as well as in models affecting B- and T-cell cross-talk [27].

To investigate the role of LIGHT in bone loss induced by estrogen deficiency, we used two approaches: demonstrating a bone phenotype in ovariectomized *Tnfsf14*$^{-/-}$ mice and quantifying LIGHT expression in women diagnosed with postmenopausal osteoporosis (PMO).

Materials and methods

Patients

The study population included 20 postmenopausal controls and 20 women affected by PMO. The clinical and demographic characteristics of the study population are shown in Table 1. The ethics committee of 'Policlinico Tor Vergata' (approval reference number 97/17), University of Rome, Rome, Italy approved all experiments described in the present study, and informed consent was obtained from all participants.

Flow cytometry on human samples

One hundred microliters of fresh EDTA peripheral blood was stained with monoclonal conjugated antibody: PE-LIGHT/TNFSF14 (clone 115 520; R&D Systems, Minneapolis, MN, USA), FITC-CD3 (clone UCHT1) and FITC-CD14 (clone M5E2; BD Pharmigen, San Diego, CA, USA). Cells were incubated for 30 min at room temperature and for another 10 min with VersaLyse reagent (Beckman Coulter, Rome, Italy) to lyse red blood cells. The same antibodies were used to evaluate LIGHT expression on peripheral blood mononuclear cells (PBMCs) cultured with or without estrogens. Flow cytometry acquisition and analysis were performed on a BD Accuri™ C6 flow cytometer (Becton Dickinson Immunocytometry System, Mountain View, CA, USA). Positivity areas were determined using an isotype-matched mAb, and a total of 2000 events for each cell sub-population were acquired.

Table 1. Clinical and demographic characteristics of the study population

	Controls	Postmenopausal osteoporosis
Number of subjects	20	20
Age (years)	48.8 ± 5.1	53.6 ± 4.4
Lumbar BMD T-score	−0.42 ± 0.44	−3.00 ± 0.51
Femoral BMD T-score	−0.27 ± 0.54	−2.54 ± 0.32

Isolation of human CD14$^+$ monocytes and CD2$^+$ T cells

PBMCs were obtained using a Histopaque 1077 density gradient (Sigma, St Louis, MO, USA). From PBMCs, CD14$^+$ and CD2$^+$ cells were purified by immunomagnetic selection (Miltenyi Biotec GmbH, Bergisch Gladbach, Germany), according to the manufacturer's instructions. Only samples with a purity greater than 98%, as checked by flow cytometry, were subjected to RNA extraction.

For some experiments, PBMCs were cultured in phenol red-free α-minimal essential medium (α-MEM; Life Technologies, Carlsbad, CA, USA) with 10% charcoal-stripped FBS (to not have estrogen in the cultures) or red α-MEM (i.e. containing phenol red) with 10% FBS for 24 and 48 h and subjected to flow cytometry to evaluate LIGHT expression.

Mice

Sibling C57bl/6 mice WT, *Tnfsf14*$^{-/-}$, and *Rag*$^-$/*Tnfsf14*$^-$ (double knockout; DKO) were obtained as described previously [10]. In brief, heterozygous *Tnfsf14*$^{+/-}$ mice were bred to produce sibling WT and *Tnfsf14*$^{-/-}$ mice. DKO mice were generated by crossing a *Rag*$^{-/-}$ homozygous mouse with a *Tnfsf14*$^{-/-}$ homozygous mouse. Subsequent generations of heterozygotes were bred together to produce a line with homozygous knockouts of both the *Rag* and the *Tnfsf14* genes. Mice were kindly provided by Professor Carl F Ware.

WT, *Tnfsf14*$^{-/-}$, and *Rag*$^-$/*Tnsf14*$^-$ mice underwent either sham surgery or ovariectomy (OVX) at 12 weeks of age and were killed at 14 weeks of age to study the acute phase of the process. Animals were housed three to four per cage at 23 °C on a 12 h:12 h light/dark cycle, and were fed a standard rodent chow and had free access to water.

For the sham or OVX surgery, mice were anesthetized by intraperitoneal injection of ketamine (100 mg/kg) and xylazine (5 mg/kg). An incision was made along the abdominal line after shaving and sterilizing. Two ovaries were carefully exteriorized and removed for the OVX group, while for the sham-operated mice, the ovaries were exteriorized and then placed back intact into the abdominal cavity. After suturing the incision, mice were treated subcutaneously with 2 mg/kg meloxicam and 5 mg/kg enrofloxacin. Mice were then returned to the

cages and their health status was monitored with daily injection of meloxicam and enrofloxacin in the following 2–3 days. At the experiment end-point, after overnight fasting, mice were euthanized by intraperitoneal injection of ketamine (100 mg/kg) and xylazine (5 mg/kg) followed by cervical dislocation and their tissues were surgically excised. The uterus of each mouse was also removed and weighed to confirm the success of OVX surgery (supplementary material, Figure S1). Left femurs were subjected to bone marrow flushing. Vertebrae and right femurs were fixed with 4% paraformaldehyde for 18 h at 4 °C and processed for histological analysis. This animal interventional study is in accordance with the European Law Implementation of Directive 2010/63/EU and all experimental protocols were reviewed and approved by the Veterinary Department of the Italian Ministry of Health.

Microcomputed tomography of femurs

Right femurs were rotated around their long axes (0.4° as rotation step) and images were acquired using a Bruker Skyscan 1172 (Bruker, Kontich, Belgium) with the following parameters: voxel size = 6 μm^3; peak tube potential = 59 kV; X-ray intensity = 167 μA; ring artefact correction = 10; beam hardening correction = 60%. Raw images were reconstructed using the SkyScan reconstruction software (NRecon) on three-dimensional cross-sectional image data sets using a three-dimensional cone beam algorithm. Structural indices were calculated on reconstructed images using the Skyscan CT Analyzer (CTAn) software (Bruker). Cortical parameters included cortical thickness (Ct.Th), total cross-sectional area (Tt. Area), cortical bone perimeter (Ct.Pm), and marrow cross-sectional area (Marrow Area). Trabecular parameters included bone volume/total volume (BV/TV), number (Tb.N), thickness (Tb.Th), separation (Tb.Sp), and diameter (Tb.Dm) dimension.

Microcomputed tomography of the spine

The fifth lumbar (L5) vertebrae of the spine were rotated around their long axes and images were acquired using a Bruker Skyscan 1172 with the following parameters: pixel size = 5 μm; peak tube potential = 59 kV; X-ray intensity = 167 μA; 0.4° rotation step. The trabecular region of the vertebral body (excluding posterior elements) was designated using manually drawn contours inside the cortical shell surrounding the entire vertebral body enclosed by the growth plates and extending for 450 6-μm slices (total 2.7 mm).

Histological analysis of bone

Femurs were embedded in methyl methacrylate (MMA) and cut using a standard microtome (RM 2155 Leica; Leica Biosystems, Heidelberg, Germany) into 5-μm-thick slices for histology. For analysis of osteoclasts (OC number per bone perimeter, N.Oc/B.Pm), bone sections were incubated in tartrate-resistant alkaline phosphatase (TRAP) staining solution; for osteoblast (OB) analysis (OB number per bone perimeter, N.Ob/B.Pm), bone sections were stained with toluidine blue. Goldner's Masson trichrome stain was used to analyze new osteoid formation. Microphotographs were captured using a light microscope (Leica) with 40× objective lens and analyzed using ImageJ software.

Cell cultures

Bone marrow (BM) was flushed from mouse femurs and tibia as follows: bones were cut at both ends with sharp sterile scissors. Using a 26-gauge needle and a 10 ml syringe filled with ice-cold PBS, bone marrow was flushed in a 50 ml Falcon conical tube. The cells obtained were centrifuged, resuspended, and cultured in α-MEM supplemented with 10% FBS and 1% penicillin/streptomycin (all from Life Technologies, Milan, Italy).

For OC differentiation, 4×10^5 bone marrow cells per cm^2 were cultured in 96-well plates (Corning GmbH, Wiesbaden, Germany) with α-MEM/10% FBS supplemented with 20 ng/ml of mouse macrophage colony-stimulating factor (MCSF; R&D Systems, Minneapolis, MN, USA) and 30 ng/ml of mouse receptor activator of nuclear factor kappa-B ligand (RANKL; R&D Systems). At day 4, mature OCs were fixed and stained for TRAP.

For osteogenic differentiation, 3×10^5 bone marrow cells were cultured in 24-well plates (Corning) with α-MEM/10% FBS supplemented with 50 μg/ml ascorbic acid and 10^{-2} M β-glycerophosphate. At day 10, cells were fixed in 3.7% (vol/vol) formaldehyde for 5 min and subjected to alkaline phosphatase (ALP) staining. To evaluate CFU-OB formation at day 20, cells were fixed and von Kossa-stained. ImageJ software was used to calculate the area of ALP$^+$ colony-forming unit fibroblasts (CFU-Fs) and CFU-OBs.

RT-qPCR

Total bone marrow RNA was extracted using spin columns (RNeasy, Qiagen, Hilden, Germany) according to the manufacturer's instructions and reverse-transcribed using iScript Reverse Transcription Supermix (Bio-Rad, Hercules, CA, USA). The resulting cDNA (20 ng) was subjected to quantitative PCR using the SsoFast EvaGreen Supermix (Bio-Rad) on an iCycler iQ5 Cromo4 (Bio-Rad) for 40 cycles (denaturation 95 °C for 5 s; annealing/extension 60 °C for 10 s) after an initial 30 s step for enzyme activation at 95 °C. Primer sequences have been previously reported [10,13]. Each transcript was assayed in triplicate and normalized to *Actb*.

Statistical analyses

Statistical analyses were performed by Student's *t*-test, non-parametric tests (Mann–Whitney for non-normal data), or ANOVA, according to the Statistical Package for the Social Sciences (IBM SPSS) software. Results were considered statistically significant at $p < 0.05$.

Results

Ovariectomy fails to cause bone loss in LIGHT-deficient mice

Wild-type (WT) and knockout (KO) mice were subjected to ovariectomy (WT-OVX, KO-OVX) or sham surgery (WT-SHAM, KO-SHAM). At sacrifice, the animals did not display significant differences in body weight (supplementary material, Figure S1A). Conversely, they showed significantly smaller uterus size and lower uterus weight in OVX mice compared to sham-operated mice, thus confirming the success of OVX (supplementary material, Figure S1B).

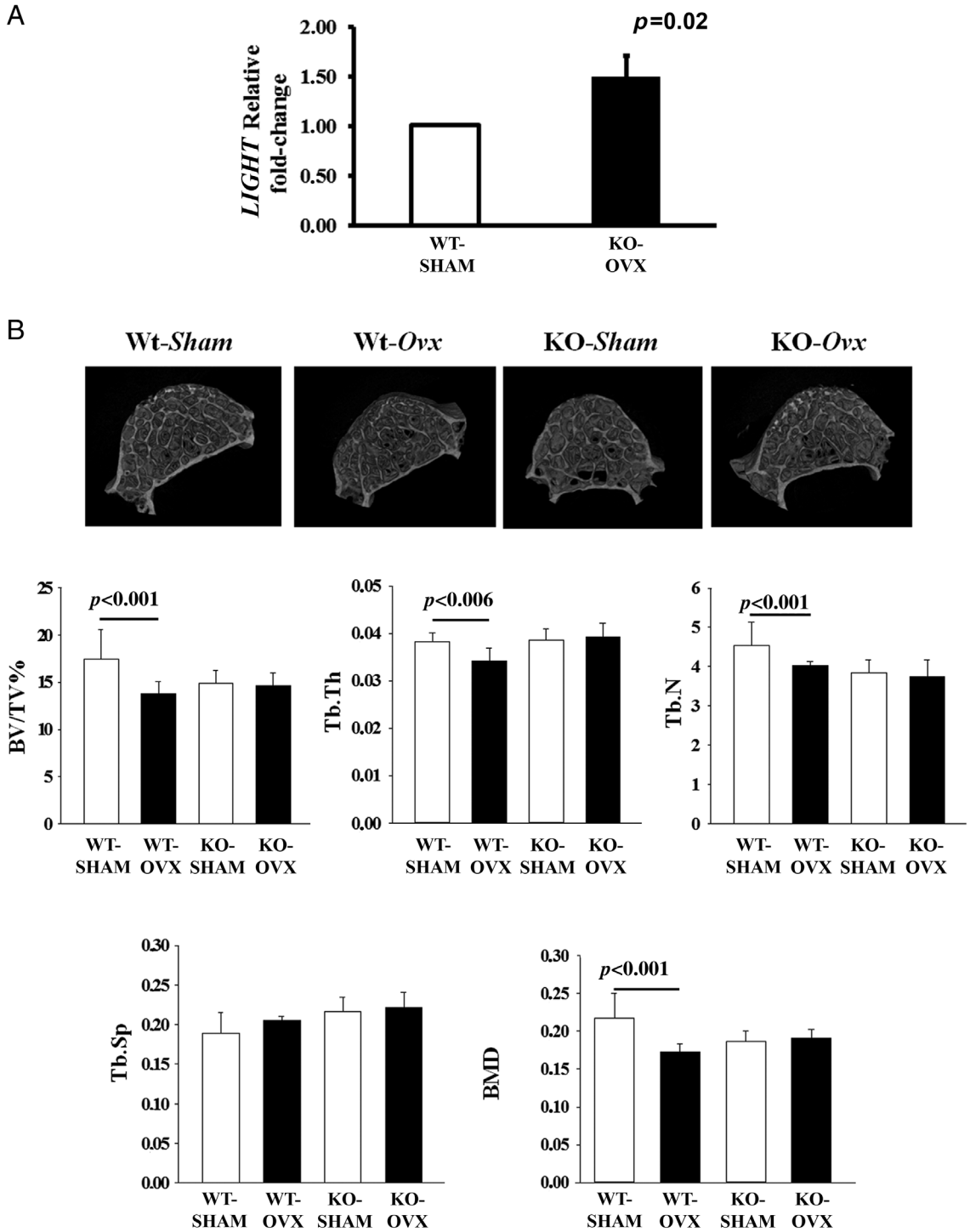

Figure 1. Effects of ovariectomy (OVX) on LIGHT expression of WT mice and on bone structure of vertebrae in WT and *Tnfsf14*-KO mice. (A) *LIGHT* mRNA levels were determined in fresh lysates of total bone marrow (BM) cells from WT-SHAM and WT-OVX mice. (B) Representative μCT-generated section images of L5 vertebra and graphs reporting calculated trabecular parameters: bone volume/total volume (BV/TV), trabecular thickness (Tb.Th), trabecular number (Tb.N), trabecular separation (Tb.Sp), and bone mineral density (BMD). Mean ± SD. Student's *t*-test. $n = 6$ mice per group. The reported *P* values refer to comparison with the corresponding sham-operated group.

We evaluated the mRNA levels of LIGHT in total bone marrow lysates from WT-SHAM and WT-OVX mice, demonstrating significantly higher levels of the transcript in the OVX group (Figure 1A).

Bone mass was analyzed by micro-computerized axial tomography (μCT) in the vertebrae and femurs from all groups. As expected, WT-OVX mice showed a significant decrease in bone mass compared with WT-SHAM mice. In contrast, KO-OVX mice were protected from bone mass loss in vertebrae and femurs (Figures 1 and 2, respectively). Analysis of L5 vertebra and bone volume/total volume (BV/TV) showed that bone mass was severely reduced by 21% in WT-OVX mice compared with WT-SHAM ($p < 0.001$), whereas ovariectomy in *Tnfsf14*$^{-/-}$ mice showed no such significant changes compared with KO-SHAM mice (Figure 1). WT-OVX mice consistently showed reduced bone mass density (BMD), trabecular thickness (Tb.Th), and trabecular number (Tb.N) with respect to WT-SHAMs, and no changes were found

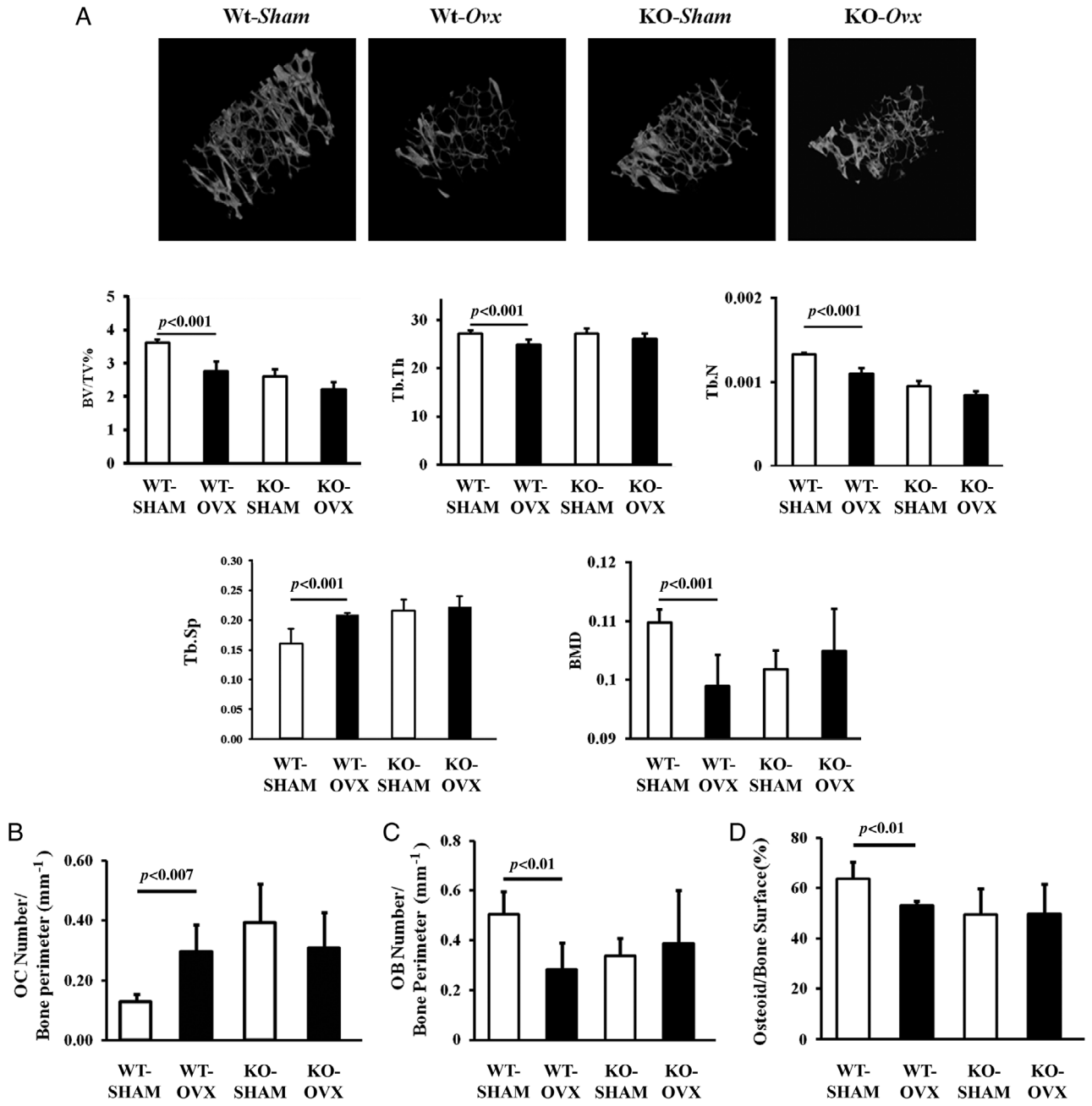

Figure 2. Effects of ovariectomy (OVX) on bone structure of femora in WT and *Tnfsf14*-KO mice. (A) Representative μCT-generated section images of trabecular bone in femora together with graphs reporting calculated trabecular parameters at the metaphysis of WT and *Tnfsf14*$^{-/-}$ mice. Trabecular bone parameters included bone volume/total volume (BV/TV), trabecular thickness (Tb.Th), trabecular number (Tb.N), trabecular separation (Tb.Sp), and bone mineral density (BMD). Also shown are (B) osteoclast and (C) osteoblast counts per bone perimeter as well as (D) osteoid/bone surface percentage in femur sections from all mice. Mean ± SD. Student's *t*-test. $n = 6$ mice per group. The reported *P* values refer to comparison with the corresponding sham-operated group.

under these parameters in ovariectomized *Tnfsf14*$^{-/-}$ and KO-SHAM mice (Figure 1). Furthermore, histomorphometry of femurs showed that the reduced cortical thickness (~8.3%, WT-SHAM 0.119 ± 0.006 versus WT-OVX 0.107 ± 0.0008, $p < 0.01$) seen in WT-OVX mice was not detected in *Tnfsf14*$^{-/-}$ mice, compared with their respective sham animals (KO-OVX 0.121 ± 0.008 versus KO-SHAM 0.120 ± 0.009). This suggests that *Tnfsf14*$^{-/-}$ prevented worsening of the cortical thickness, which was also associated with the significantly reduced tissue mineral density seen in WT-OVX mice compared with the sham controls (WT-OVX 0.76 ± 0.02, $p < 0.04$ versus WT-SHAM 0.81 ± 0.03); furthermore, these deteriorations were not evident in the *Tnfsf14*$^{-/-}$ mice (KO-OVX, $p < 0.02$ versus KO-SHAM 0.81 ± 0.03). Although ovariectomy lowered femoral trabecular bone mass density (~10.90%, $p < 0.01$), BV/TV, Tb.Th, and Tb.N, and increased trabecular spacing (Tb.Sp) in WT-OVX mice with respect to their sham-operated controls, we detected no such differences when ovariectomy was performed in *Tnfsf14*$^{-/-}$ mice compared with the ovariectomized shams (Figure 2A). In addition, when femoral trabecular bone was analyzed histomorphometrically to assess the numbers of osteoclasts and osteoblasts per bone perimeter, TRAP-positive osteoclast number significantly increased and osteoblastic epithelioid cells per bone perimeter decreased in WT-OVX mice compared with sham controls and KO-OVX mice (Figure 2B, supplementary material, Figure S2A, Figure 2C, and supplementary material, Figure S2B, respectively). Consistently, in WT-OVX mice, the percentage of osteoids per bone surface was significantly reduced compared with the WT-SHAMs, whereas no significant changes were detected between KO-OVX and KO-SHAM mice (Figure 2D and supplementary material, Figure S2C).

Ovariectomy in *Tnfsf14*$^{-/-}$ mice increases CFU fibroblasts, CFU osteoblasts, and osteoclast formation

Because ovariectomy increases the proliferation of stromal cells [27], we investigated the ability of *Tnfsf14*$^{-/-}$ mice to form alkaline phosphatase-positive colonies required for stromal commitment to osteoblastic lineage in the bone marrow. As expected, the number of early osteoblast precursor colonies, revealed as CFU-Fs, and the amount of mineralized nodule formation, shown as CFU-OBs, increased approximately two-fold in bone marrow samples from WT-OVX mice, compared with the WT-SHAM (Figure 3A). By contrast, ovariectomy in *Tnfsf14*$^{-/-}$ mice had no effects on the number of either CFU-Fs

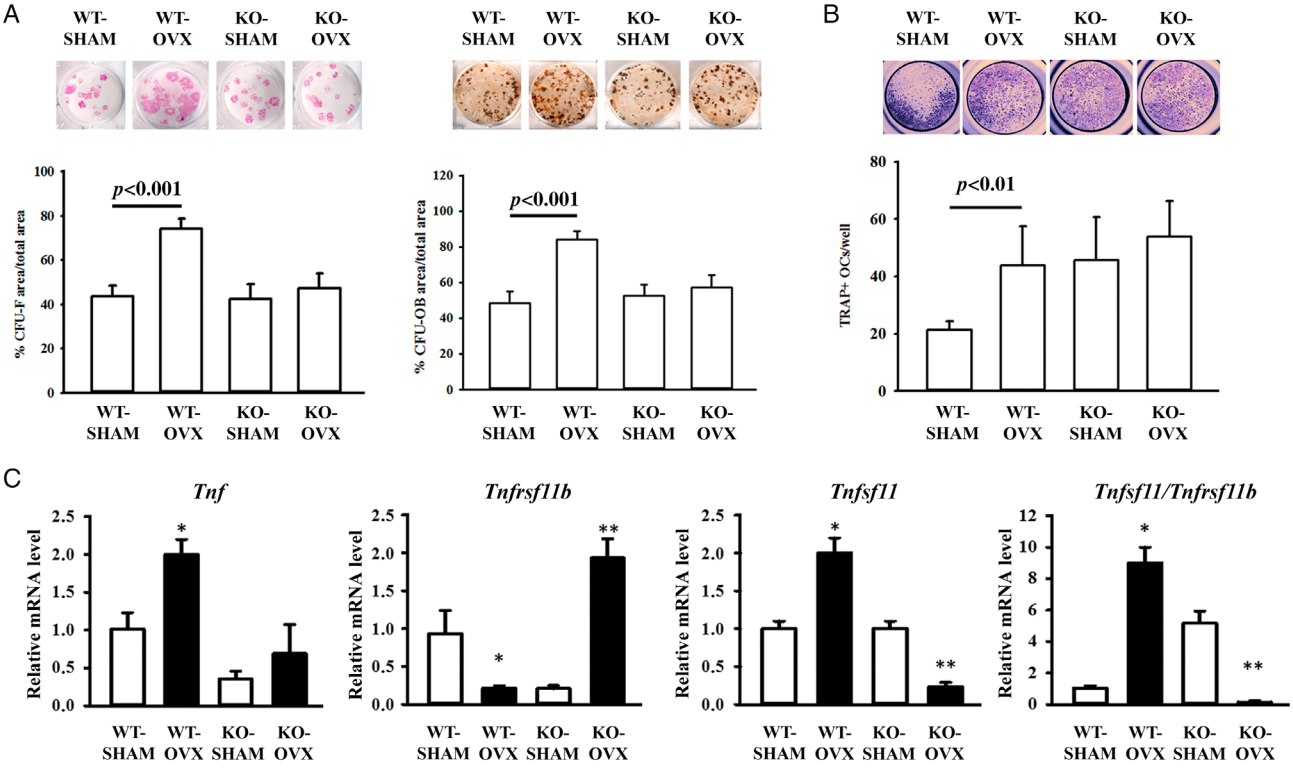

Figure 3. Effects of ovariectomy (OVX) in *ex vivo* cultures and cytokine expression in WT and *Tnfsf14*-KO mice. Bone marrow stromal cells from all mice were grown in osteoblast differentiation medium. (A) The percentage of alkaline phosphatase-positive CFU-F colonies (10 days) and von Kossa-positive mineralized CFU-OB colonies (21 days) from WT mice was calculated. Representative wells are shown. (B) Representative images for tartrate-resistant acid phosphatase (TRAP)-stained cell cultures derived from all mice together with OC counts. (C) *Tnf*, *Tnfrsf11b*, and *Tnfsf11* mRNA levels, together with the *Tnfsf11*/*Tnfrsf11b* ratio, were determined using fresh lysates of total bone marrow (BM) cells. Original magnification: 1×. Student's *t*-test. $n = 6$ mice per group. The reported *P* values refer to comparison with the corresponding sham-operated group.

or CFU-OBs (Figure 3A), suggesting that ovariectomy can impair osteogenic potential through *Tnfsf14*$^{-/-}$. In *ex vivo* bone marrow cell cultures from the same animals, once again we found that osteoclastogenesis was significantly increased in WT-OVX mice, while ovariectomy did not change the number of osteoclasts in *Tnfsf14*$^{-/-}$ mice, compared with those from sham surgeries (Figure 3B). These findings suggest that when estrogen is deficient, LIGHT is required to generate a bone marrow microenvironment with high osteoclastogenic activity.

Subsequently, we used total bone marrow extracts to evaluate cytokine expression in osteoclastogenesis, such as *Tnf*, *Tnfrsf11b*, and *Tnfsf11*, by RT-qPCR (Figure 3C). WT-OVX mice showed a two-fold increase of TNFα compared with WT-SHAM, whereas *Tnf* levels, although somewhat increased, were not statistically different in KO-OVX mice compared with KO-SHAM. The two-fold increase in *Tnfsf11*, and abruptly reduced *Tnfrsf11b* levels induced by ovariectomy in WT-OVX mice, had completely reversed in KO-OVX mice compared with KO-SHAMs (Figure 3C), leading to a higher *Tnfsf11/Tnfrsf11b* ratio in WT-OVX compared with KO-OVX mice ($p < 0.0001$). This may explain why knockout mice are protected from ovariectomy-induced bone loss.

Ovariectomy increases femoral bone mass in *Rag*$^{-/-}$*Tnfsf14*$^{-/-}$ double-knockout mice

It is known that ovariectomy determines B- and T-cell proliferation, and we previously demonstrated that these cells are involved in trabecular bone loss associated with *Tnfsf14*$^{-/-}$ deficiency. Therefore, we looked deeper into the role of both LIGHT and B and T cells in OVX by operating on *Rag*$^{-/-}$*Tnfsf14*$^{-/-}$ DKO mice arising from the breeding of *Tnfsf14*$^{-/-}$ onto *Rag*$^{-/-}$ mice, a strain that does not develop mature T or B cells [28]. Interestingly, by analyzing L5 vertebra, μCT analysis showed no significant differences in BV/TV, Tb.Th, Tb.N, or Tb.Sp in DKO-OVX mice compared with DKO sham-operated mice (not shown). Similarly, μCT analysis showed no significant differences in the femur cortical compartment of DKO-OVX mice compared with sham

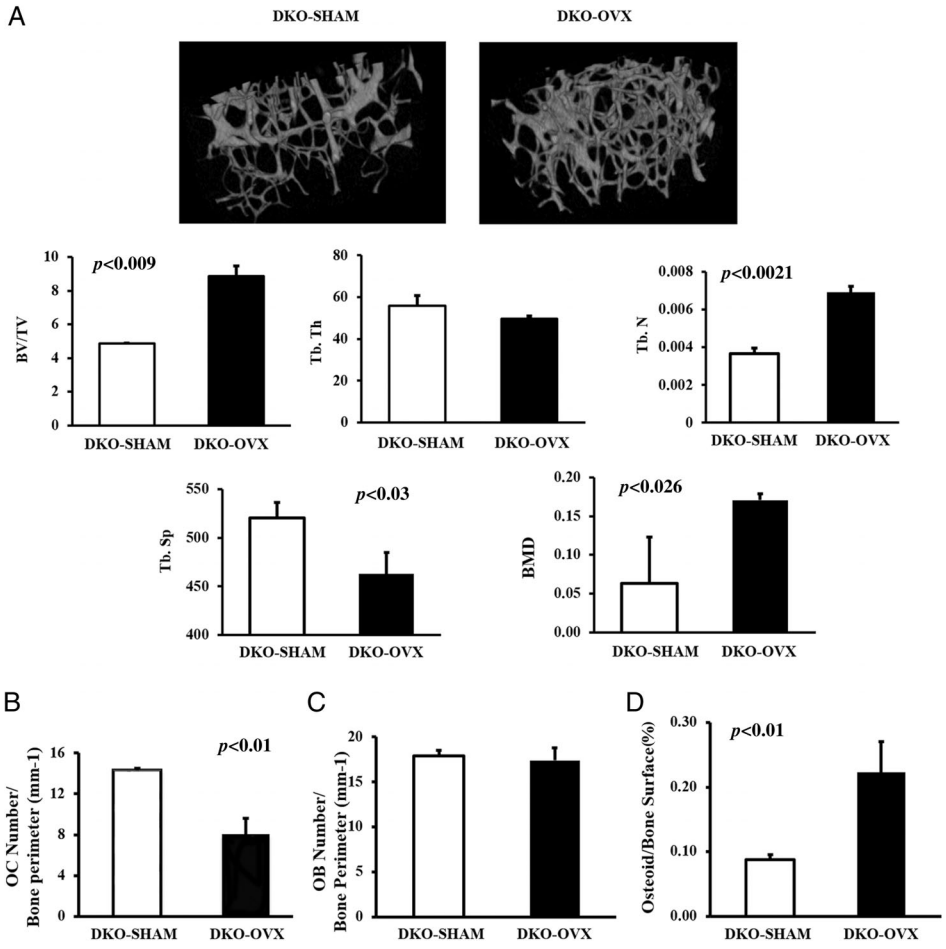

Figure 4. Effects of ovariectomy (OVX) on bone structure of femora in DKO mice. (A) Representative μCT-generated section images of trabecular bone in femora together with graphs reporting calculated trabecular parameters at the metaphysis of DKO mice. Trabecular bone parameters included bone volume/total volume (BV/TV), trabecular thickness (Tb.Th), trabecular number (Tb.N), trabecular separation (Tb.Sp), and bone mineral density (BMD). Also shown are (B) osteoclast and (C) osteoblast counts per bone perimeter, as well as (D) osteoid/bone surface percentage in femur sections from all mice. Mean ± SD. Student's *t*-test. $n = 6$ mice per group. The reported *P* values refer to comparison with the corresponding sham-operated group.

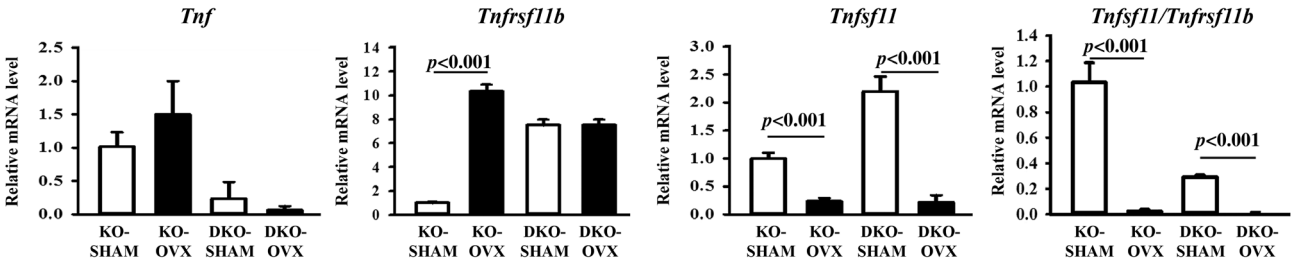

Figure 5. Effects of ovariectomy (OVX) on TNFα, OPG, and RANKL expression in DKO mice. *Tnf*, *Tnfrsf11b*, and *Tnfsf11* mRNA levels, together with the *Tnfsf11*/*Tnfrsf11b* ratio, were determined in fresh lysates of total bone marrow (BM) cells of DKO-SHAM and DKO-OVX mice. Student's *t*-test. $n = 6$ mice per group. The reported *P* values are referred to the corresponding sham-operated group.

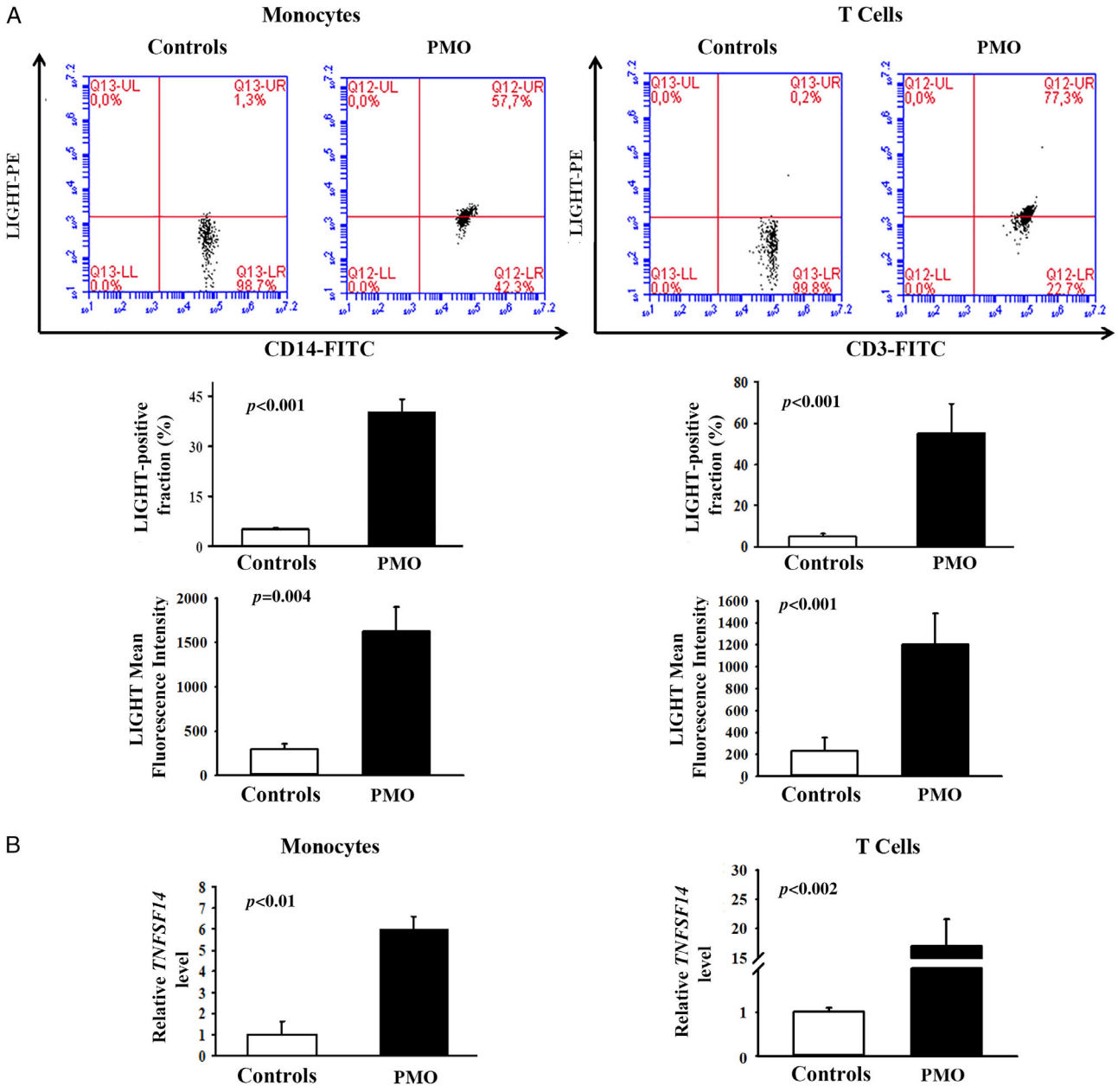

Figure 6. LIGHT expression in postmenopausal patients. Higher LIGHT expression in postmenopausal osteoporosis (PMO) was detected on $CD14^+$ monocytes and $CD3^+$ lymphocytes by (A) flow cytometry and (B) RT-qPCR compared with the controls.

operated mice (data not shown). In the femurs of DKO-OVX mice, ovariectomy triggered a significant increase of trabecular bone, as demonstrated by a 50% increase in trabecular BV/TV ($p < 0.009$), a 50.6% ($p < 0.002$) increase in Tb.N, and a 15% ($p < 0.03$) decrease in Tb. Sp. Thus, bone mineral density increased in DKO-

OVX mice compared with the DKO-SHAM mice (Figure 4A). Yet again, histomorphometric analysis of femora demonstrated that osteoclast numbers were significantly reduced ($p < 0.01$, Figure 4B and supplementary material, Figure S3A) when induced by ovariectomy in DKO mice, whereas osteoblast numbers per bone perimeter showed no significant difference compared with sham surgeries (Figure 4C and supplementary material, Figure S3B). The percentage of osteoids per bone surface also significantly increased in DKO-OVX mice compared with DKO-SHAM mice (Figure 4D and supplementary material, Figure S3C). Furthermore, when we assessed *Tnf*, *Tnfrsf1b*, and *Tnfsf11* levels in total bone marrow extracts of DKO-OVX and OVX-SHAM mice (Figure 5), the *Tnf* and *Tnfrsf1b* levels did not differ in either the DKO-OVX or the DKO-SHAM mice, although both were significantly reduced compared with the KO-SHAM ($p < 0.01$ and $p < 0.001$). Of note, DKO-OVX mice showed strongly decreased *Tnfsf11* levels, compared with DKO-SHAM mice, and consistently had the lowest *Tnfsf11*/*Tnfrsf11b* ratio. Consequently, in bone disease associated with ovariectomy, the LIGHT effect is mainly mediated by T and B cells via changes in cytokine expression that target bone cell activity.

LIGHT expression in postmenopausal patients

We next investigated LIGHT levels on immune cells in 20 women with postmenopausal osteoporosis (PMO) and 20 healthy females as controls (Table 1).

Using flow cytometry, we analyzed LIGHT expression in monocytes and T cells from the peripheral blood of patients and controls. A significantly higher percentage of LIGHT levels was seen for both cell types in the PMO patients compared with the controls (Figure 6A). Using RT-qPCR, we demonstrated that the mRNA level for this cytokine was also elevated in isolated monocytes and T cells from patients with PMO compared with the controls (Figure 6B). We also evaluated by flow cytometry LIGHT expression on PBMCs from healthy donors with or without estrogens for 24 and 48 h. We did not find significant differences for the cytokine expression between the two conditions on $CD14^+$ and $CD3^+$ cells (data not shown). These findings suggest that LIGHT's possible involvement in the pathogenesis of bone loss is induced by estrogen withdrawal (menopause).

Discussion

Here, we demonstrated that LIGHT deficiency *in vivo* combined with T- and B-depleted cells reduced the capability of acute estrogen deficiency to promote osteoblast and osteoclast differentiation that determines bone loss. We also reported that LIGHT is important for ovariectomy to enhance *Tnf* levels and the *Tnfsf11*/*Tnfrsf11b* ratio. Additionally, we showed that in patients with postmenopausal osteoporosis, LIGHT is overexpressed in circulating cells. These findings suggest a prominent function for T-, B-, and bone-cell interplay in the mechanism through which ovariectomy determines bone loss.

In 2006, Edwards *et al* first demonstrated in rheumatoid arthritis that LIGHT (a co-stimulatory molecule) is involved in erosive bone disease [8]. We then deepened the understanding of LIGHT's role in bone remodeling in the pathologies of multiple myeloma, lung cancer, CKD, and alkaptonuria [9,11–13,29]. In 2018, we studied the bone phenotype of $Tnfsf14^{-/-}$ mice and demonstrated trabecular bone loss, suggesting that a physiological basal concentration of LIGHT is required to maintain physiological bone remodeling [10]. Here, we report that $Tnfsf14^{-/-}$ mice are protected from bone loss induced by ovariectomy. Nevertheless, we cannot exclude that the lack of bone loss in $Tnfsf14^{-/-}$ mice following ovariectomy might be dependent on the fact that there is low bone mass in the naïve mice. However, a similar behavior has been described for another co-stimulatory cytokine, CD40L. In fact, it has already been shown that *Cd40l*-deficient mice displayed reduced bone mass and these same mice are protected from bone loss induced after estrogen withdrawal [27]. Also, *Cd40l*-deficient mice displayed complete defense against bone resorption enhancement, typical of ovariectomy-induced bone loss, together with inhibition of TNFα increased expression and decrease of the RANKL/OPG ratio that develops after estrogen withdrawal in bone marrow cells [27].

Here, we also found that $Tnfsf14^{-/-}$ deficiency inhibits the stimulatory outcomes of ovariectomy on CFU-Fs and osteoclastogenesis. Specifically, we showed that LIGHT is necessary following ovariectomy to enhance the capability of bone marrow cells by sustaining osteoclastogenesis through increased production of *Tnf* and *Tnfsf11*, and reduced *Tnfrsf11b* expression. Furthermore, CFU-Fs from $Tnfsf14^{-/-}$ mice failed to react to ovariectomy by augmenting osteoblasts to proliferate and differentiate. Although $Tnfsf14^{-/-}$ mice did not display alterations in the B-cell and $CD4^+$ T-cell compartments but only $CD8^+$ T cells displayed proliferative defects with normal cytotoxic function [30,31], we previously demonstrated that these cells are involved in trabecular bone loss associated with $Tnfsf14^{-/-}$ deficiency [10]. Therefore, we looked deeper into the role of both LIGHT and B and T cells in ovariectomy by operating on DKO mice that simultaneously lack LIGHT, B and T cells. Thus, we demonstrated that together with LIGHT, B and T cells played a prominent role. Our DKO mice were protected from ovariectomy-induced bone loss, thus displaying increased femoral BV/TV, Tb.N, and bone mineral density, as well as decreased osteoclastogenesis. These events are associated with reduced *Tnf* levels and *Tnfsf11*/*Tnfrsf11b* ratio in bone marrow cells, which further substantiates the essential role of T and B cells in bone loss associated with ovariectomy.

Estrogens are noteworthy in their ability to modulate bone mass [32]. Using animal models, it has been

demonstrated that the cross-talk of immune mediators and bone cells determines, either in part or completely, bone loss associated with estrogen withdrawal [33]. T cells are involved in bone loss linked to estrogen withdrawal [23]. In fact, in nude mice and rats displaying severe T-cell deficiency, bone loss did not occur after estrogen withdrawal [23,34]. Ovariectomy supports T-cell activation through antigen enhancement [35,36] and augments thymus output of T cells into peripheral blood [37]. Ovariectomy is also associated with increased T-cell proliferation and lifespan in the bone marrow [26,35]. Th17 cells increase after ovariectomy and promote osteoclastogenesis by producing IL-17 [38], which in turn stimulates osteoblasts to produce pro-osteoclastogenic cytokines, such as IL-6, TNFα, and RANKL. Additionally, ovariectomy enhances TNFα production by T cells, thus increasing RANKL-induced osteoclastogenesis [23]. This outcome is due to both an augmented number of TNFα-producing T cells [24] and the increased secretion of TNFα per cell [27,39]. Additionally, ovariectomy enhances the percentage of senescent $CD4^{+}CD28^{-}$ T cells [39], which secrete high TNFα levels. TNFα- and p55 TNF receptor-deficient mice are protected from ovariectomy-induced bone loss [24]. Furthermore, T-cell involvement in producing TNFα has been supported by demonstrating *in vivo* that replacing bone marrow in nude recipient mice with T cells from WT mice rescues the ability of ovariectomy to induce bone loss; when T cells are replaced in TNFα-deficient mice, this induction fails [24].

B-cell ontogenesis is also augmented by estrogen withdrawal [40], and the literature suggests that the relationship between B cells and bone cells participates in part due to bone loss associated with estrogen withdrawal [41]. In mouse bone marrow, ovariectomy enhances the number of RANKL-expressing B cells [42]. RANKL-deficient mice in B cells were partly protected from the loss of trabecular bone induced by ovariectomy [43]. All these literature data demonstrating the partial or total protection from bone loss associated with ovariectomy in mice lacking B or T cells, together with our previous findings demonstrating that DKO mice display a significant increase of trabecular bone structure with respect to $Rag^{-/-}$ mice [10], can explain our choice to evaluate the effect of ovariectomy only on DKO mice.

All the results obtained from our mouse models of estrogen withdrawal strongly support our findings, which show high LIGHT levels in monocytes and T cells from patients with postmenopausal osteoporosis. Interestingly, LIGHT expression by these cells did not change on culturing them with or without estrogens, thus suggesting that the increase of LIGHT in postmenopausal osteoporosis patients is due to a complex scenario, involving different cells of the bone marrow milieu. The central role of immune cells in postmenopausal osteoporosis has been consistently demonstrated in humans [15]. D'Amelio *et al* demonstrated a crucial role for T cells in postmenopausal bone loss. Specifically, the authors reported that *in vitro* osteoclast formation from circulating precursors takes place only in cultures with T cells, which were more active than controls [44]. Indeed, postmenopausal T cells express high levels of TNFα and RANKL, thus supporting osteoclastogenesis [44]. Additionally, in postmenopausal osteoporosis, high RANKL levels in marrow stromal cells and lymphocytes were associated with the enhanced markers of bone resorption and with the circulating estrogen concentration [45].

In conclusion, we highlight that acute estrogen deficiency alters osteoblastogenesis and osteoclastogenesis through the T-cell co-stimulatory receptor LIGHT. Understanding this mechanism may produce new pharmacological strategies to counteract bone loss associated with postmenopausal osteoporosis.

Acknowledgements

We thank FFARB, Department of Basic and Medical Sciences, Neurosciences and Sense Organs (Contributo Residuo Ricerca Scientifica Ex 60% Progetti Anno 2015), and the University of Bari (Ministero dell'Istruzione Università e Ricerca) (ex 60% grant; to GB).

Author contributions statement

GB conceived and designed the study. GS performed most of the experiments. AO performed flow cytometry and contributed to cell cultures and statistical analysis. MC, UT, and GP provided patients' samples and clinical data. GC and MF performed statistical analysis. MDC and GI contributed to histology. JER performed microCT analysis. CFW provided mice and critically revised the manuscript. MG and SC participated in experiment design and critical revision of the manuscript. All the authors read and approved the final version of the manuscript.

References

1. Šedý J, Bekiaris V, Ware CF. Tumor necrosis factor superfamily in innate immunity and inflammation. *Cold Spring Harb Perspect Biol* 2014; **7:** a016279.
2. Gommerman JL, Browning JL, Ware CF. The lymphotoxin network: orchestrating a type I interferon response to optimize adaptive immunity. *Cytokine Growth Factor Rev* 2014; **25:** 139–145.
3. Steinberg MW, Cheung TC, Ware CF. The signaling networks of the herpesvirus entry mediator (TNFRSF14) in immune regulation. *Immunol Rev* 2011; **244:** 169–187.
4. Ware CF, Sedý JR. TNF superfamily networks: bidirectional and interference pathways of the herpesvirus entry mediator (TNFSF14). *Curr Opin Immunol* 2011; **23:** 627–631.
5. Mauri DN, Ebner R, Montgomery RI, *et al*. LIGHT, a new member of the TNF superfamily, and lymphotoxin α are ligands for herpesvirus entry mediator. *Immunity* 1998; **8:** 21–30.
6. Tamada K, Shimozaki K, Chapoval AI, *et al*. LIGHT, a TNF-like molecule, costimulates T cell proliferation and is required for

dendritic cell-mediated allogeneic T cell response. *J Immunol* 2000; **164:** 4105–4110.
7. Holmes TD, Wilson EB, Black EV, *et al*. Licensed human natural killer cells aid dendritic cell maturation via TNFSF14/LIGHT. *Proc Natl Acad Sci U S A* 2014; **111:** E5688–E5696.
8. Edwards JR, Sun SG, Locklin R, *et al*. LIGHT (TNFSF14), a novel mediator of bone resorption, is elevated in rheumatoid arthritis. *Arthritis Rheum* 2006; **54:** 1451–1462.
9. Brunetti G, Rizzi R, Oranger A, *et al*. LIGHT/TNFSF14 increases osteoclastogenesis and decreases osteoblastogenesis in multiple myeloma-bone disease. *Oncotarget* 2014; **5:** 12950–12967.
10. Brunetti G, Faienza MF, Colaianni G, *et al*. Impairment of bone remodeling in LIGHT/TNFSF14-deficient mice. *J Bone Miner Res* 2018; **33:** 704–719.
11. Brunetti G, Tummolo A, D'Amato G, *et al*. Mechanisms of enhanced osteoclastogenesis in alkaptonuria. *Am J Pathol* 2018; **188:** 1059–1068.
12. Cafiero C, Gigante M, Brunetti G, *et al*. Inflammation induces osteoclast differentiation from peripheral mononuclear cells in chronic kidney disease patients: crosstalk between the immune and bone systems. *Nephrol Dial Transplant* 2018; **33:** 65–75.
13. Brunetti G, Rizzi R, Storlino G, *et al*. LIGHT/TNFSF14 as a new biomarker of bone disease in multiple myeloma patients experiencing therapeutic regimens. *Front Immunol* 2018; **9:** 2459.
14. D'Amelio P. The immune system and postmenopausal osteoporosis. *Immunol Invest* 2013; **42:** 544–554.
15. Henning P, Ohlsson C, Engdahl C, *et al*. The effect of estrogen on bone requires ERα in nonhematopoietic cells but is enhanced by ERα in hematopoietic cells. *Am J Physiol Endocrinol Metab* 2014; **307:** E589–E595.
16. Weitzmann MN, Pacifici R. Estrogen deficiency and bone loss: an inflammatory tale. *J Clin Invest* 2006; **116:** 1186–1194.
17. Nakamura T, Imai Y, Matsumoto T, *et al*. Estrogen prevents bone loss via estrogen receptor alpha and induction of Fas ligand in osteoclasts. *Cell* 2007; **130:** 811–823.
18. Krum SA, Miranda-Carboni GA, Hauschka PV, *et al*. Estrogen protects bone by inducing Fas ligand in osteoblasts to regulate osteoclast survival. *EMBO J* 2008; **27:** 535–545.
19. Martin-Millan M, Almeida M, Ambrogini E, *et al*. The estrogen receptor-α in osteoclasts mediates the protective effects of estrogens on cancellous but not cortical bone. *Mol Endocrinol* 2010; **24:** 323–334.
20. Jilka RL, Takahashi K, Munshi M, *et al*. Loss of estrogen upregulates osteoblastogenesis in the murine bone marrow. Evidence for autonomy from factors released during bone resorption. *J Clin Invest* 1998; **101:** 1942–1950.
21. Kousteni S, Bellido T, Plotkin LI, *et al*. Nongenotropic, sex-nonspecific signaling through the estrogen or androgen receptors: dissociation from transcriptional activity. *Cell* 2001; **104:** 719–730.
22. Kousteni S, Han L, Chen JR, *et al*. Kinase-mediated regulation of common transcription factors accounts for the bone-protective effects of sex steroids. *J Clin Invest* 2003; **111:** 1651–1664.
23. Cenci S, Weitzmann MN, Roggia C, *et al*. Estrogen deficiency induces bone loss by enhancing T-cell production of TNF-alpha. *J Clin Invest* 2000; **106:** 1229–1237.
24. Roggia C, Gao Y, Cenci S, *et al*. Up-regulation of TNF-producing T cells in the bone marrow: a key mechanism by which estrogen deficiency induces bone loss *in vivo*. *Proc Natl Acad Sci U S A* 2001; **98:** 13960–13965.
25. Gao Y, Qian WP, Dark K, *et al*. Estrogen prevents bone loss through transforming growth factor beta signaling in T cells. *Proc Natl Acad Sci U S A* 2004; **101:** 16618–16623.
26. Gao Y, Grassi F, Ryan MR, *et al*. IFN-gamma stimulates osteoclast formation and bone loss *in vivo* via antigen-driven T cell activation. *J Clin Invest* 2007; **117:** 122–132.
27. Li JY, Tawfeek H, Bedi B, *et al*. Ovariectomy disregulates osteoblast and osteoclast formation through the T-cell receptor CD40 ligand. *Proc Natl Acad Sci U S A* 2011; **108:** 768–773.
28. Mombaerts P, Iacomini J, Johnson RS, *et al*. RAG-1-deficient mice have no mature B and T lymphocytes. *Cell* 1992; **68:** 869–877.
29. Brunetti G, Belisario DC, Bortolotti S, *et al*. LIGHT/TNFSF14 promotes osteolytic bone metastases in non-small cell lung cancer patients. *J Bone Miner Res* 2019. https://doi.org/10.1002/jbmr.3942 [Epub ahead of print].
30. Liu J, Schmidt CS, Zhao F, *et al*. LIGHT-deficiency impairs $CD8^+$ T cell expansion, but not effector function. *Int Immunol* 2003; **15:** 861–870.
31. Tamada K, Ni J, Zhu G, *et al*. Cutting edge: selective impairment of $CD8^+$ T cell function in mice lacking the TNF superfamily member LIGHT. *J Immunol* 2002; **168:** 4832–4835.
32. Khosla S, Riggs BL. Pathophysiology of age-related bone loss and osteoporosis. *Endocrinol Metab Clin North Am* 2005; **34:** 1015–1030.
33. Riggs B. Endocrine causes of age-related bone loss and osteoporosis. *Novartis Found Symp* 2002; **242:** 247–259.
34. Sass D, Liss T, Bowman AR, *et al*. The role of the T-lymphocyte in estrogen deficiency osteopenia. *J Bone Miner Res* 1997; **12:** 479–486.
35. Cenci S, Toraldo G, Weitzmann MN, *et al*. Estrogen deficiency induces bone loss by increasing T cell proliferation and lifespan through IFN-γ-induced class II transactivator. *Proc Natl Acad Sci U S A* 2003; **100:** 10405–10410.
36. Adamski J, Ma Z, Nozell S, *et al*. 17β-Estradiol inhibits class II major histocompatibility complex (MHC) expression: influence on histone modifications and CBP recruitment to the class II MHC promoter. *Mol Endocrinol* 2004; **18:** 1963–1974.
37. Ryan MR, Shepherd R, Leavey JK, *et al*. An IL-7-dependent rebound in thymic T cell output contributes to the bone loss induced by estrogen deficiency. *Proc Natl Acad Sci U S A* 2005; **102:** 16735–16740.
38. Tyagi AM, Srivastava K, Mansoori MN, *et al*. Estrogen deficiency induces the differentiation of IL-17 secreting Th17 cells: a new candidate in the pathogenesis of osteoporosis. *PLoS One* 2012; **7:** e44552.
39. Tyagi AM, Srivastava K, Sharan K, *et al*. Daidzein prevents the increase in $CD4^+$CD28null T cells and B lymphopoiesis in ovariectomized mice: a key mechanism for anti-osteoclastogenic effect. *PLoS One* 2011; **6:** e21216.
40. Masuzawa T, Miyaura C, Onoe Y, *et al*. Estrogen deficiency stimulates B lymphopoiesis in mouse bone marrow. *J Clin Invest* 1994; **94:** 1090–1097.
41. Katavić V, Grčević D, Lee SK, *et al*. The surface antigen CD45R identifies a population of estrogen-regulated murine marrow cells that contain osteoclast precursors. *Bone* 2003; **32:** 581–590.
42. Kanematsu M, Sato T, Takai H, *et al*. Prostaglandin E2 induces expression of receptor activator of nuclear factor-kappa B ligand/osteoprotegrin ligand on pre-B cells: implications for accelerated osteoclastogenesis in estrogen deficiency. *J Bone Miner Res* 2000; **15:** 1321–1329.
43. Onal M, Xiong J, Chen X, *et al*. Receptor activator of nuclear factor κB ligand (RANKL) protein expression by B lymphocytes contributes to ovariectomy-induced bone loss. *J Biol Chem* 2012; **287:** 29851–29860.
44. D'Amelio P, Grimaldi A, Di Bella S, *et al*. Estrogen deficiency increases osteoclastogenesis up-regulating T cells activity: a key mechanism in osteoporosis. *Bone* 2008; **43:** 92–100.
45. Eghbali-Fatourechi G, Khosla S, Sanyal A, *et al*. Role of RANK ligand in mediating increased bone resorption in early postmenopausal women. *J Clin Invest* 2003; **111:** 1221–1230.

SUPPLEMENTARY MATERIAL ONLINE

Figure S1. Effect of ovariectomy (OVX) on body and uterus weights in WT and *Tnfsf14*-KO mice

Figure S2. Effect of ovariectomy (OVX) on bone cells of femora in WT and *Tnfsf14*-KO mice

Figure S3. Effect of ovariectomy (OVX) on bone cells of femora in DKO mice

75 Years ago in *The Journal of Pathology…*

Two cases of mixed malignant tumour of the breast

A. D. Telford Govan

Malignant tubular adenoma in a horseshoe kidney: Its significance with regard to general cancer pathology

Peter Ladewig, Sati Eser

A microscopical study of the evolution of mouse mammary cancer: The effect of the milk factor and a comparison with the human disease

Georgiana M. Bonser

The use of the splenectomised rabbit for the assay of liver extracts; with observations on the chemical nature of the anti-pernicious anæmia factor

W. Jacobson, S. M. Williams

Arrhenoblastoma: Report of a case with unusual features

B. Jolles, H. H. Gleave

To view these articles, and more, please visit:
www.thejournalofpathology.com

Click 'BROWSE' and select 'All issues', to read articles going right back to Volume 1, Issue 1 published in 1892.

The Journal of Pathology
Understanding Disease

A Journal of The Pathological Society